Int J Adv Manuf Technol (2016) 86:977–988
DOI 10.1007/s00170-015-8255-z

ORIGINAL ARTICLE

A novel force rendering approach for virtual assembly of mechanical parts

Q. H. Wang[1] · Z. D. Huang[1] · J. L. Ni[1] · W. Xiong[1] · J. R. Li[1]

Received: 4 July 2015 / Accepted: 16 December 2015 / Published online: 30 December 2015

Abstract Virtual assembly (VA) is a typical virtual reality (VR)-based application in engineering. However, common interaction devices, such as keyboard and mouse, are less realistic due to lack of force sensation. Therefore, realistic force feedback in the VA environment provides a more natural interaction to simulate the assembly operation and result in improved task efficiency. This paper presents a novel force rendering approach, which focuses on mechanical part assembly based on three basic mechanical fit types, namely clearance fit, interference fit, and transition fit. The algorithm to calculate the assembly force is formulated by analyzing the tolerance variation along the assembly length between two mating parts. And then the force is rendered continuously at real-time during the VA operation to provide a fast, stable, and more realistic assembly force feedback to the users. Several comparative case studies are conducted to investigate the approach with the users' performance of VA with the other three common approaches, namely conducting assembly task using a WIMP-based CAD software, with a standard physically based approach and the one with both collision detection and geometric constraints, respectively. The proposed approach is more efficient than other approaches by providing continuous force feedback to the users so as to greatly enhance their force sensation of the assembly operation. Moreover, case studies on users' identification capability of different fit types has shown that with the continuous force rendering, users can easily tell the clearance fit from the other two fit types, hence the proposed approach equips users with the ability to possibly evaluate the assembly performance at the early stage of product development process.

Keywords Virtual assembly · Force rendering · Tolerance and fit

✉ J. R. Li
lijr@scut.edu.cn

[1] School of Mechanical and Automotive Engineering (SMAE), South China University of Technology, Guangzhou, Guangdong, China

1 Introduction

Virtual assembly (VA) is a typical virtual reality (VR)-based application in engineering. It can be defined as "the use of computer tools to make or assist with assembly-related engineering decision through analysis, predictive models, visualization, and presentation of data with physical realization of the production or supporting process." [1]. Different from conventional CAD software that overlooks assembly processes, VA offers users an approach to assemble virtual representations of physical models through simulating a realistic environment behavior and to validate the assembly performance of products early in the product development process ahead of any physical prototyping [2]. Moreover, it can provide a more natural human–machine interaction to enhance human performance during assembly task execution. However, how to simulate interaction realistically in VA operations has been a challenging problem for both research and industrial community. Common interaction devices, such as keyboard and mouse, are less realistic due to lack of force sensation, and therefore they cannot provide VA application a natural interaction solution to simulate the assembly operation and sensation that the operator perceived in the real assembly process. On the other hand, haptics technology offers a revolutionary solution for realistic interaction in virtual environment, with which users can feel and manipulate virtual objects by using special input/output devices to get tactile and force feedback [3].

Research has shown that the addition of haptics to virtual environments result in improved task efficiency [4, 5]. Force cues provided by haptics technology can help users feel and better understand the virtual objects by supplementing visual and auditory cues and creating an improved sense of presence in the virtual environment [6–8]. Many researchers have spared no efforts to integrate this new technology into VA simulation. And several prototype systems have been developed: Coutee et al. [9] designed a haptic integrated dis/re-assembly analysis (HIDRA) using a dual PHANTOM setup and demonstrated that force feedback is helpful for virtual assembly and disassembly interaction. Seth et al. [10, 11] developed a VA system named SHARP for haptic assembly and realistic prototyping. They applied physically based modeling for simulating realistic part behavior and provided an intuitive dual-handed PHANTOM haptic interface for mechanical assembly in an immersive VR environment. Iglesias et al. [12] developed a peer-to-peer collaborative haptic assembly system, which permits two users to haptically and simultaneously interact with the same virtual scene to undertake assembly and maintenance operations.

According to statistics, mechanical assembly takes up over 60 % of total assembly work of products. It means that the quality of final products highly depends on the quality of assembly operations and processes [13, 14]. In mechanical assemblies, individual components are placed together to deliver a certain function. While the performance, quality, and cost of a mechanical assembly are significantly affected by its tolerances [15]. During the course of assembly operations, with different tolerance levels, the assembly forces to be used differ. In other words, a precise assembly operation needs to apply accurate forces to ensure the quality of assembly, which is indeed an important factor of product quality. Several force rendering approaches have been proposed to compute and generate forces in response to user interactions with virtual objects. Garbaya et al. [16] carried out a study focusing on contact force rendering and the concept of spring-damper model was adopted to preclude the interpenetration of parts during their mating phase of the virtual assembly. Xia et al. [3] presented a real-time attractive force and repulsive force rendering algorithm to realize the mating or inserting process during the assembly simulation stage. However, most of these force feedback approaches used simplified part model representations and were based on spring-damper models to get crude force values in order to maintain the update rate requirements (~1 kHz) of the hardware in VR applications. The lack of concern on part shape accuracies causes problem that it is hard for users to distinguish the different tolerance levels of the assembling parts in the virtual environment, which in turn reduces the sense of reality. Furthermore, without a realistic feeling of the assembly force, the evaluation and simulation of the mechanical assembly cannot be conducted effectively.

This paper proposes a novel force rendering approach to provide real-time assembly force feedback during the mating phase of a mechanical assembly operation. The assembly force calculation is based on three assembly fit types, namely clearance fit, interference fit, and transition fit. It provides users a more realistic and interactive feeling of virtual assembly.

The remainder of this paper is organized as follows: related terminologies are introduced in Section 2. Then, the assembly force rendering approach and the force calculation algorithms for different fit types are discussed in Section 3. In the following section, Section 4, design of prototype system and case studies are presented with discussions, while the last section, Section 5, concludes the work.

2 Terminologies

For mechanical products, the key geometry feature of a part is defined by its specified dimensions known as basic sizes or nominal sizes. However, the final dimensions of the part vary within a permissible deviation from the specified basic sizes, known as tolerance, due to reasons such as manufacturing process errors, setup errors, and other uncertain factors. The proper functioning of a machine depends on the tolerances specified for its parts, particularly those that must fit together for location or for suitable relative motion. Generally, there are three fit types defined based on the relative looseness or tightness of mating parts. Clearance fit refers to the design case where there must always be a clearance between mating parts; transition fit is used where accuracy of location is important, but a small amount of clearance or a small amount of interference is acceptable; while interference fits are those in which the inside member is larger than the outside member, requiring the application of force during assembly [17]. For each fit type, standard tolerance classes are provided for designers to choose. Different tolerance classes within each fit type also indicate the looseness or tightness of the assembly. Therefore, in order to allow users to conduct a more realistic virtual assembly operation, the parts' mating tolerance should be taken into account for force rendering.

2.1 Tolerance control factor

Due to the machining error generated from many factors in actual manufacturing processes, for a specific part, its dimension varies within a small range, which is defined by its fit type and tolerance class designed. In other words, during the assembly operation, the assembly tolerance would not be a constant but a variable instead at different location of the mating surfaces. Accordingly, the assembly force needed for the operation would also vary with the varying assembly tolerance. Therefore, in order to simulate the assembly force more

realistically, on top of the actual part's dimension, which is measured by the quality control engineer at a few selected location of the part, the randomized change of the surface dimension along the assembly mating length is defined as *tolerance control factor* $B(l_i)$ here and is represented as:

$$B(l_i) = (1-\alpha)B(l_j) + \alpha B(l_{j+1}) \quad l_j \le l_i < l_{j+1},$$
$$\alpha = \frac{l_i - l_j}{l_{j+1} - l_j} \tag{1}$$

where

$$B(l_j) = \frac{k}{2} * \text{random}(-1, 1) \tag{2}$$

$$l_j = \frac{jL}{N}, j = 1, 2, 3, \ldots, N \tag{3}$$

For a continuous and stable VA simulation, a linear interpolation algorithm is used to calculate the tolerance control factor $B(l_i)$. l_i denotes the assembly length corresponding to the time t_i during VA simulation. It is between two adjacent sample assembly lengths, $l_j \le l_i < l_{j+1}$. $B(l_j)$ is calculated by a random function to simulate the randomized surface dimension on the assembly length l_j, which is one of the sample assembly lengths; N is an integer that represents the total number of the assembly lengths sampled; and k represents the amplitude of random value decided by the surface roughness. Here, for simplification, we assume that both of the mating surfaces are manufactured with same machining accuracy, hence the maximum heights of profile Rz of both assembling surfaces are identical. Then, the approximate value of k is taken as Rz for simulation.

2.2 Assembly clearance space

In this work, the concept of *assembly clearance space* (ACS) is defined to describe the assembly tolerance variation between two mating parts. Due to the quality constraints of machining processes, which are mainly related to machine tool precision and experiences of human operators, at different section along the assembly direction or assembly length, the tolerance of two mating parts would vary within a small range. Therefore, take a typical case of shaft-bushing assembly for example, the value of ACS can be calculated by the difference between the two parts' respective radial dimension along the mating surface.

As shown in Fig. 1, the bushing has a thru-hole while the shaft has a solid cylinder with the same basic size, i.e., $D = d$. The assembly operation is to mount the bushing onto the shaft so that the hole and cylinder share the same axis and the bushing is secured along axial direction by the shaft shoulder. The key design parameters of this mating are the hole diameter of the bushing, noted as D_{EI}^{ES}, and the shaft diameter at the mating section, d_{ei}^{es} (Fig. 1a); as a basic rule for mechanical assembly, the basic sizes of these two parts are identical, i.e., $D = d$ but their tolerances vary. As shown in Fig. 1b, the ACS at radial direction is the free space that the shaft can move around within the hole of the bushing. Moreover, to simplify the calculation, the area of ACS can be calculated by the free moving space of the shaft axis. It is a small circular area whose center is the bushing center and the radius is the eccentricity, i.e., between the centers of the shaft and bushing.

Since the bushing is to be mounted onto the shaft along its axial direction with an assembly length of L, therefore, along L, at each of every sections perpendicular to the shaft axis, i.e., at different l_i, due to the variations of actual dimension of the hole and cylinder surface, ACS varies. Mathematically, a function $S(l_i)$ is proposed to describe the variation of ACS and defined as follows:

$$S(l_i) = \left(\frac{D_h}{2} - \frac{d_s}{2}\right) + B(l_i) \tag{4}$$

Where $S(l_i)$ denotes the radius of ACS section at the corresponding assembly length l_i along the assembly length L, D_h and d_s are the actual diameters of bushing hole and shaft cylinder, respectively, and $B(l_i)$ is the tolerance control factor defined above. For a particular batch of same parts, research has found out that the actual dimension of these parts follows a normal distribution [18]. To be more clear, taking the shaft diameter d_s as an example, if the shaft diameter is taken as $10_{0.000}^{0.012}$, then the value of d_s can be obtained through simulation using a discrete normal distribution whose probability mass function (pmf) is defined as $\text{pmf}(x) = \Pr(x - 0.5 < X \le x + 0.5)$ for $x \in Z$, where X is normally distributed with the mean $\mu = 6$ and the standard deviation $\sigma = 2$ and Z denotes the set of integers $\{0, 1, 2, 3, \ldots, 12\}$ [15].

For each of fit types, due to the looseness or tightness of the mating surfaces defined, the distribution of $S(l_i)$ is different, as shown in Fig. 2. The value of $S(l_i)$ would vary within the range determined by the maximum clearance S_{max}, and the minimum clearance S_{min}, which equals to be $ES - ei$ and $EI - es$, respectively. For clearance fit (Fig. 2a), the value of $S(l_i)$ is positive all the time, which indicates a clearance between mating surfaces, while for interference fit (Fig. 2b), its value would be negative all the time indicating interference. For transition fit (Fig. 2c), the distribution is more complicated, and the value of $S(l_i)$ could be either positive or negative.

2.3 Virtual assembly force

In VA simulation, in order to improve operators' perception and immersion during virtual operations, providing a realistic force feedback to the operator is necessary. A *virtual assembly force* is the kind of force perceived by the operator when two parts get into mating during the assembly process. As a

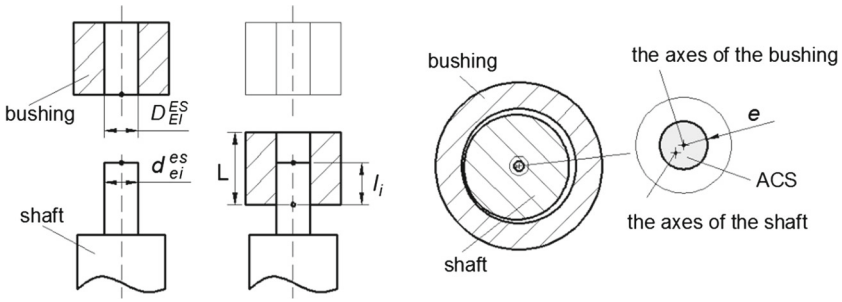

(a) The assembly process of bushing-shaft mating (b) The radial section of ACS

Fig. 1 Illustration of ACS with a bushing-shaft assembly

general practice, the total assembly force can be divided into three force components in Cartesian coordinates, namely F^x, F^y, and F^z according to the effect of the assembly operation. Take the common mechanical assembly of a shaft and a bushing for example, as shown in Fig. 3, F^x and F^y are the radial assembly forces generated from the contact between parts' surfaces. They constrain the part from moving toward the X and Y direction; while the axial force F^z is the frictional force between parts' surfaces, it is the minimum force needed for assembly along the shaft axis.

The virtual assembly force feedback to the operator should be a continuous and changing force, which is calculated based on the possible surface tolerance variation at the particular location during the assembly operation. Different assembly fit type needs different virtual assembly force calculation method, which would be discussed in detail in the next section.

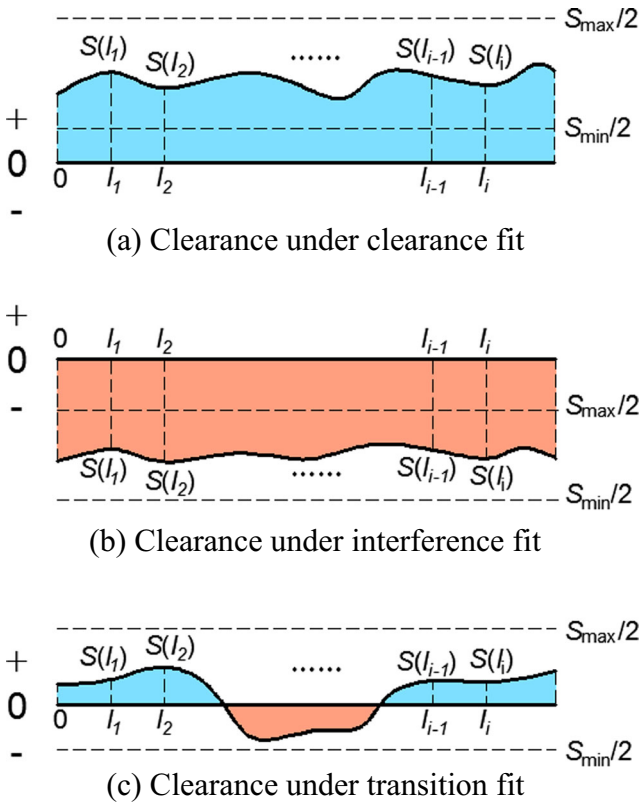

Fig. 2 Illustration of the distribution of ACS radius with three fit types. **a** Clearance under clearance fit, **b** clearance under interference fit, and **c** clearance under transition fit

3 Virtual assembly force rendering

In VA simulation, there are many research works [16] reported on analyzing the geometric constraints of the particular mating of parts and then applying a constant spring-damper model-based resistance force to simulate the constraint feeling along the assembly direction during the mating. This kind of resistance force is ideal for the high update rate requirement of VA applications and haptic devices, but certainly less realistic and immersive in terms of user's perception. Moreover, due to lack of considering the effect of the surface tolerance information, users cannot distinguish the assembly mating condition for different fit types, and hence it is difficult to evaluate the assembly or the design for its operability. In this work, a novel virtual assembly force rendering algorithm based on three mechanical fit types is proposed. It analytically simulates and calculates the assembly force at every mating position during assembly process while avoiding time-wasting collision detection and maintaining the high update rate requirement for VA at the same time.

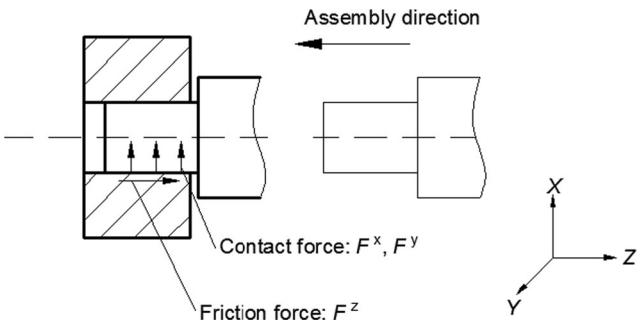

Fig. 3 Illustration of virtual assembly force of a shaft-bushing assembly operation

3.1 Virtual assembly force calculation of two mating surfaces under a clearance fit

As mentioned in previous section, the value of $S(l_i)$ would be all positive for two surfaces with a clearance fit, which means there is a clearance between mating surfaces. As shown in Fig. 4a, therefore, along X and Y direction, at any assembly time t_i, as long as the radial offset Δd_i is within the ACS, i.e., $\Delta d_i \leq S(l_i)$, the operator could then assemble the shaft into the hole without any constraint. Only if when the center point of shaft section, which is controlled by the operator through the haptic device interface, is moved outside of the area of ACS, i.e., $\Delta d_i > S(l_i)$, as shown in Fig. 4b, then the shaft would be physically in contact with the hole. This contact during the assembly operation is common in actual assembly case, hence such contact force is implemented by a common mass-spring model and feedback to the operator. On the other hand, the axial assembly force F^z acting as a frictional force is calculated on the basis of the Coulomb friction model. So the algorithm can be described as follows:

$$\begin{cases} F_i^x = \begin{cases} k_p \ (\Delta d_i - \overset{0}{S}(l_i)) \ \cos\theta_i & \Delta d_i \leq S(l_i) \\ 0 & \Delta d_i > S(l_i) \end{cases} \\ F_i^y = \begin{cases} k_p \ (\Delta d_i - \overset{0}{S}(l_i)) \ \sin\theta_i & \Delta d_i \leq S(l_i) \\ 0 & \Delta d_i > S(l_i) \end{cases} \\ F_i^z = \mu\sqrt{\left(F_i^x\right)^2 + \left(F_i^y\right)^2} \qquad S(l_i) > 0 \end{cases} \tag{5}$$

Where θ_i denotes the angle between the radial offset and X-axis; k_p represents stiffness coefficient, its value is obtained empirically by testing different values until the dynamic behavior of the virtual part becomes stable and smooth; and μ is the coefficient of friction between the mating surfaces.

3.2 Virtual assembly force calculation of two mating surfaces under an interference fit

For two mating surfaces under an interference fit, the value of $S(l_i)$ would be all negative, which means that the shaft is constrained to be align with the hole. Therefore, the assembly force is a resistance force activated for the entire assembly time to restrict the shaft of its axial motion. Then the axial assembly force of interference fit can be considered as the minimum force needed for axial assembly on the basis of the thick-cylinder theory and Coulomb friction model. Considering a uniform distribution of contact pressure and both parts of unique materials, the minimum assembly force needed is then given by:

$$F = \mu 2\pi R \int_0^L p(l)dl \tag{6}$$

Where μ is the coefficient of friction between the two mating surfaces, R is half of the basic or nominal diameter of the mating shaft/hole, and l is the assembly length ranging from 0 to L. And the contact pressure $p(l)$ is a function of the radial interference $S(l)$:

$$p(l) = \frac{ES(l)}{2R}\left(1-c_0^2\right) \tag{7}$$

Where E is the Young's modulus decided by the material property of the model, c_0 represents the radius ratio R/r_0, and r_0 represents the outer radius of the mating hole. So, the virtual assembly force of interference fit can be described as follows:

$$\begin{cases} F_i^x = k_q \Delta x_i \\ F_i^y = k_q \Delta y_i \\ F_i^z = F_{i-1}^z + k_r \mu \pi E\left(1-c_0^2\right)\Delta l_i S(l_i) \end{cases} \tag{8}$$

Where Δx_i and Δy_i denote the offset distance between device position and shaft-bushing center along X-axis and Y-axis at time t_i, respectively, Δl_i is the assembly length over the time period from t_{i-1} to t_i, k_q represents linear stiffness for the axis constraint, and k_r is the scale coefficient that used to map the assembly force calculated to the force display range of the haptic device interface.

3.3 Virtual assembly force calculation of two mating surfaces under a transition fit

For transition fits, the value of $S(l_i)$ along the assembly length could be positive or negative. To simplify the problem, the cases when the actual variation of the ACS is all positive (a

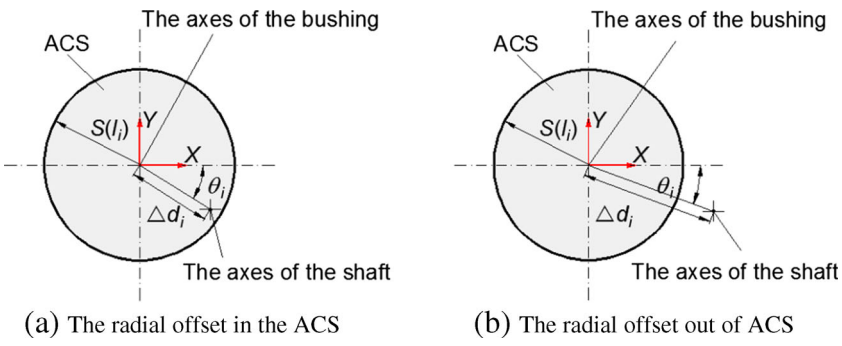

Fig. 4 Illustration of the radial offset during the assembly operation

clearance indeed) or all negative (an interference fit actually) are already discussed, hence, the assumption is made that only when the value of $S(l_i)$ is fluctuating around zero, then the simulation is effective, so as the shaft is constrained to be aligned with the hole and a resistance force in radial direction will be activated. In the axial direction, the axial assembly force F^z is calculated and accumulated only when the value of $S(l_i)$ is below zero. As a summary, the virtual assembly force of transition fits can be described as follow:

$$\begin{cases} F_i^x = k_q \Delta x_i \\ F_i^y = k_q \Delta y_i \\ F_i^z = \begin{cases} F_{i-1}^z & S(l_i) \geq 0 \\ F_{i-1}^z + k_s \mu \pi E \left(1 - c_0^2\right) \Delta l_i \delta(l_i) & S(l_i) < 0 \end{cases} \end{cases} \quad (9)$$

Where k_s represents the scale coefficient, like the k_r above, to map the force magnitude to the display range of the haptic device interface.

4 Case studies

The simulation of the assembly task in the virtual environment requires a high level of user perception acquired by natural and intuitive interaction [19]. During a virtual task, the manipulation of parts with specific 3D interaction devices has important effect on the user performance and the corresponding sensation of realism [20, 21]. For testing the usability of the proposed virtual assembly force rendering approach and the user performance during the assembly task, a prototype VA system is designed, as shown in Fig. 5a, and six sets of experiments are carried out.

4.1 Prototype system design

The prototype VA environment runs on an Intel E3-1230 (3.3 GHz) PC with Windows 7 operating system. The PC is with 8 GB of memory and a NVIDIA GTX750Ti graphics card. The haptic device used in this work is PHANTOM Desktop from Sensable Technologies®. The software infrastructure of the prototype VA environment was built using C++ as the programming language and Microsoft Visual Studio 2012 as the development environment. As shown in Fig. 5b, by the haptic interaction point (HIP), operator can explore the virtual environment and get the force feedback during VA operations through the haptic device. The application is launched into three separate threads: haptics thread, physics thread, and graphics thread. Among them, the haptic thread, launched by the OpenHaptics toolkit, is responsible for force rendering and communicating with the haptic device, which is executed at a higher frequency (~1000 Hz); the physics thread uses Bullet, an open source physics engine, to perform all the collision detection and dynamics calculations for simulating realistic part behavior. Its update rate is controlled at 100 Hz; while the graphics thread uses OpenGL as the graphic engine for visualizing the entire graphics scene by the built-in display list function and runs at a lower frequency of about 30 Hz.

4.2 Design of case studies

4.2.1 Procedure and subjects

In order to test the prototype system, six experimental conditions of a typical shaft (part A) and bushing (part B) assembly are designed in the VA environment. Among them, there are three referential cases, i.e., A1, A2, and A3, which are without assembly force rendering, and the other three cases, i.e., B1, B2, and B3, are with assembly force sensation of different assembly fit types. For a better comparison, the assembly task for each case is an identical insertion operation as shown in Fig. 5a. The user needs to complete the insertion of shaft-part A into the bushing-part B located on the chuck. The basic diameters of shaft and bushing here are both selected as ∅40 mm, while the length of the bushing is 50 mm.

The operating procedure is as follows:

Step 1 The user grasps part A by the HIP and explores the VA environment (Fig. 6a).
Step 2 The user or system moves part A toward part B and complete the parts' axial alignment.
Step 3 The user or system should insert part A into part B along the assembly length until the shaft reaches its final assembly location at the other end of the bushing; the distance d_1 is of a very small value near to zero (Fig. 6c).

For evaluating the usability of proposed approach, a heuristic evaluation method, which is a popular usability inspection method in the field of human–computer interaction [22], is adopted here. In this work, more specifically, evaluators (the experiment participants) are involved to examine the haptic interface and judging its compliance with the three evaluation factors (the "heuristics") for VA of mechanical parts. The three factors are:

(1) Immersion of the VA system: measure how much feeling of presence the user can perceive with the virtual operations with and without assembly force sensation.
(2) Identification ability of different fit types: measure if the user can distinguish the difference among fit types by the virtual assembly operation.
(3) Stability and continuity of assembly force feedback: measure if the user can feel the assembly force naturally and stably.

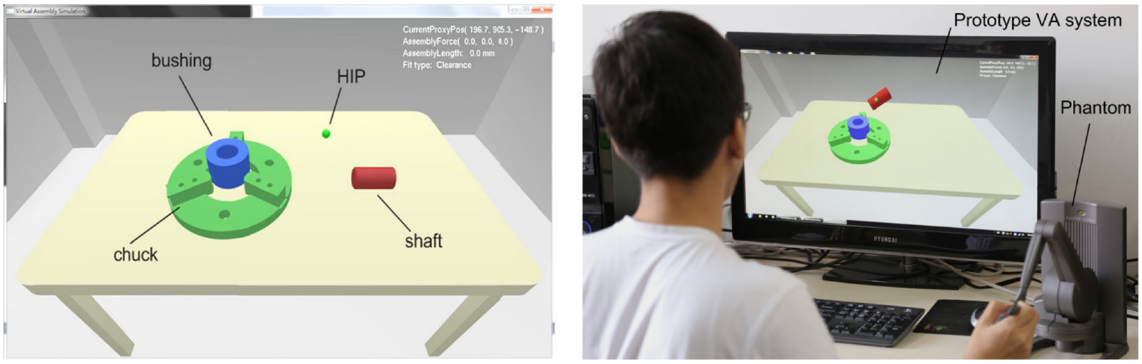

(a) The scene of the prototype VA system (b) Assembly task in the VA environment

Fig. 5 Prototype system setup. **a** The scene of the prototype VA system; **b** assembly task in the VA environment

Fifteen participants were invited to conduct the experiment. All of them have basic understanding about haptic technology and VA simulation. Moreover, before the experiments, each participant received an intensive training session about half an hour on the assembly operation with the prototype system so as to get familiarized with the experiment setup. And then all of them were asked to carry out the assembly task under every experimental condition.

4.2.2 Experiment A1, A2, and A3 without assembly force rendering

Experiments A1, A2, and A3 are designed as reference case studies, in which the participants perform the insertion assembly task without assembly force rendering. In the experiment A1, the participants need to perform the assembly task using a WIMP interface based on popular CAD software, SolidWorks®. The assembly task is performed by adding geometric constraint to two parts with the built-in assembly function of the software. In the experiment A2, the participants are asked to perform the task in the prototype VA environment with the collision detection only, which is provided through the physics thread. More specifically, during the assembly process, collision detection is activated to prevent parts' penetration with a resistance force. While in experiment A3, besides collision detection, geometric constraints are also provided during the process to improve the assembly efficiency. In general, two geometric constraints, i.e., (1) axis orientation constraint and (2) face match constraint [23], are mainly used in computer-aided design software for assembly operations and hence are adopted in virtual assembly operations as well. When the angle and distance between two assembling parts' axes are in proximity ($\theta \leq 10°, d_0 \leq 5\text{mm}$), the collision detection is deactivated and axis orientation constraint is activated. And then the system restricts part A to move along axial direction. At this condition, the system recognizes the beginning of the insertion. When part A is moved to a position very close to the pre-defined final assembly position ($d_1 \leq 3\,\text{mm}$), the face matching constraint is activated and an audio feedback would be played to inform the users that it is the end of the assembly operation. In these experiments, the assembly tolerance are all selected as H7/g6, which means that the assembly operation is performed under the condition of a clearance fit. For the other two fit types, i.e., transition and interference fits, since there is actual contact between two parts' mating surfaces due to the tolerance design, the contact detection would lead to the result that the shaft part would penetrate with the bushing all the time during the entire insertion operation. Since the force feedback is calculated by the degree of penetration, which turns to be uncontrollable and instable due to

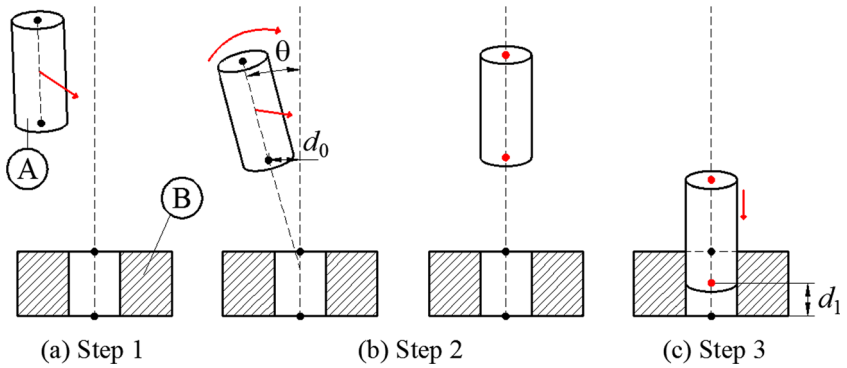

Fig. 6 The operation steps of the bushing and shaft product assembly. **a** Step 1, **b** step 2, and **c** step 3

the delay between the system calculation and user's perception. The end result would be that the user holds the shaft part and feels its vibrating up and down within the ACS. Therefore, it makes no sense to conduct referential cases with these two fit types.

4.2.3 Experiments B1, B2, and B3 with assembly force rendering

Experiments B1, B2, and B3 request the participants to conduct the same insertion assembly task; however, the tolerance design defines the mating of shaft and bushing with three different fit types: clearance fit, interference fit, and transition fit, respectively. Similar with the experiment A3, once the angle and distance of parts' axes are in proximity, the collision detection is deactivated and simultaneously the proposed assembly force approach is activated in these experiments to provide assembly force feedback during step 3 of the experiment procedure.

In these experiments, the material of shaft and bushing are both selected as same steel with the Young's modulus E = 210 GPa and the coefficient of friction $\mu = 0.15$. The outer diameter of bushing is 80 mm. The assembly tolerance of three fit type are selected as *H*7/*g*6, *H*7/*p*6, and *H*7/*k*6 corresponding to the experiments B1, B2, and B3. The maximum heights of profile Rz is selected as 6.3 μm for each experiment. Then the tolerance control factor $B(l_i)$ of each experiment is generated randomly based on the selected assembly tolerance and Rz. The stiffness coefficients k_p and k_q of two parts are chosen as 700 and 500 N/m, respectively. Due to the device constraint that the maximum output force of the PHANTOM Desktop is fixed, thus we used the scale coefficients k_r and k_s to map the actual calculated assembly force to the force range that the device can output.

4.3 Discussions

4.3.1 The user performance of the proposed algorithm

In order to test the user performance of the assembly operation, each participant was requested to repeat five times for the assembly task with the same fit type in experiments A1, A2, A3, and B1. The time to completion (TTC) of each experiment was recorded and shown as Fig. 7. The results show that the average TTC is 26.73 s for case B1, 15.06 s for case A1, 49.78 s for case A2, and 24.58 s for case A3. From the results, it can be found that the average TTC for case A1 is the least, which is due to the simplest assembly operation in CAD software as there is no physics or force feedback during the process. Comparing with the physically based VA approach, i.e., experiment A2, the proposed approach is better in terms of TTC. This is a promising performance indicator since the proposed approach allows the user to conduct the identical assembly operation faster; hence, the efficiency of VA is better. Moreover, the approach implements not only physics-related effect but also the continuous force feedback during the operation. As illustrated by the following evaluation, with this force feedback, the users' sensation in VA is greatly enhanced. To compare with the operating time of A3, i.e., assembly under physical modeling and geometric constraint as well, the proposed approach, i.e., experiment B1, is not significantly different. However, it adds on the feature of continuous force feedback to the user during the assembly, which is certainly a bonus point.

4.3.2 The virtual assembly force rendering

During step 3, the assembly force information is recorded by the system. Figure 8 reflects a set of assembly

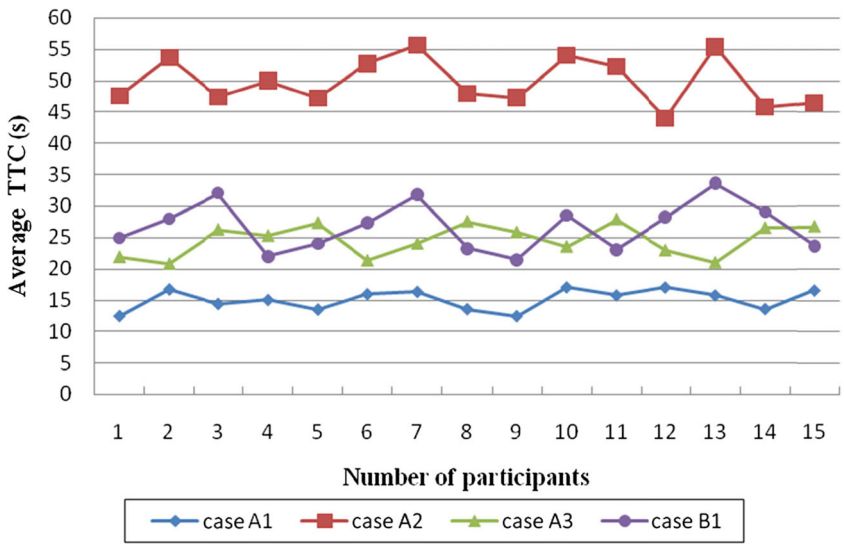

Fig. 7 Average completion time through the assembly task

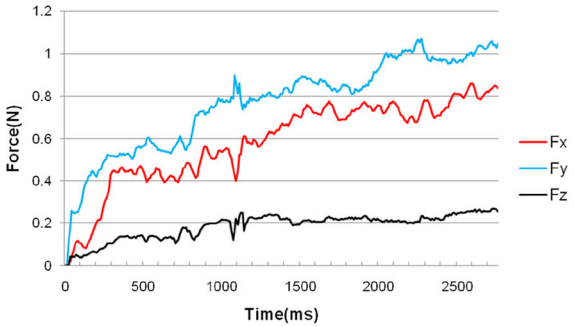

(a) Assembly force feeedback measured during Experiment B1 (cleearance fit)

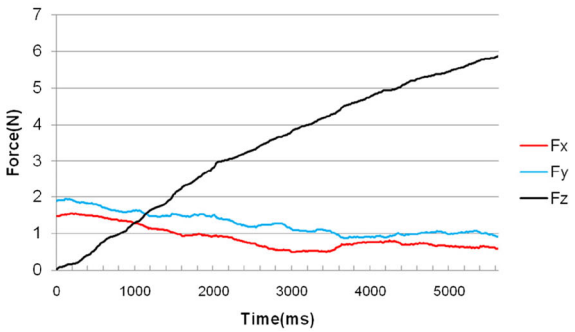

(b) Assembly force feeedback measured during Experiment B2 (interrference fit)

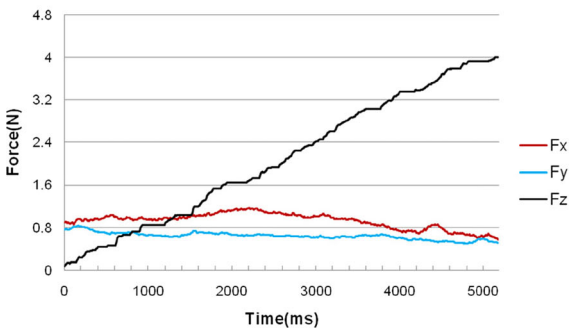

(c) Assembly force feedback measured during Experiment B3 (transition fit)

Fig. 8 Assembly force measured during the assembly task with three different fit types. **a** Assembly force feedback measured during experiment B1 (clearance fit). **b** Assembly force feedback measured during experiment B2 (interference fit). **c** Assembly force feedback measured during experiment B3 (transition fit)

forces arisen by completing the assembly operation under different fit types. In the figure, the horizontal axis reflects the operation time, while the vertical coordinate is the force feedback recorded.

With experiment B1, the two mating parts are with a clearance fit, i.e., there is a clearance between the two mating surfaces, hence during the insertion, the collision between the two cylindrical surfaces plays an important role in the force measured; as shown in Fig. 8a, the force curve of X and Y directions represent the collision force generated during the insertion. While the force output along the axial direction, F^{ε}, depends on Coulomb friction, hence the axial assembly force is relatively a small constant value, ranging from 0 to near 0.3 N.

Table 1 Heuristic evaluation

No.	Evaluation factor	Min	Max	Average
1	Immersion of the shaft-bushing assembly without assembly force feedback (experiment A3)	5	7	6.3
2	Immersion of the shaft-bushing assembly with assembly force feedback in general (experiments B1, B2, and B3)	7	9	8.5
3	Identification of different fit types with assembly force feedback (experiments B1, B2, and B3)	7	9	8.1
4	Stability and continuity of assembly force feedback (experiments B1, B2, and B3)	6	9	7.8

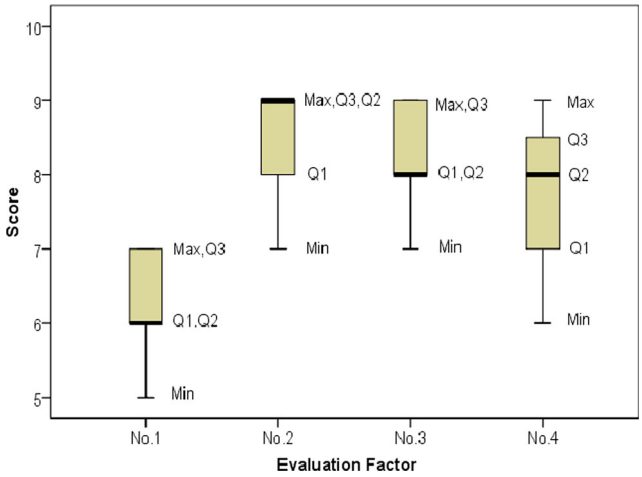

Fig. 9 Box-plot of the scores of evaluation factors

With experiments B2 and B3, the forces along X and Y directions both acted as a resistance force to prevent the movement of the shaft from its axial motion since the shaft is constrained to be aligned with the bushing during step 3 in both experiments. However, the curve of axial assembly force, F^e, is different between the experiments B2 and B3. On the one hand, it can be easily noticed that the axial assembly force under interference fit is ranging from 0 to 6 N, while the force under transition fit is just ranging from 0 to 4 N. This is because of different scale coefficients, k_r and k_s, that are used to improve users' perception of distinguishing the assembly operation under interference fit and transition fit. Furthermore, since the axial assembly force F_i^e under transition fit is calculated and accumulated only when the value of $S(l_i)$ is below zero, the curve of axial assembly force under interference fit is relatively smooth, comparing with that under transition fit, which appears to be a kind of stair-step shape.

From the force rendering data collected for all the three fit types, it can be seen that the prototype is able to provide a stable force in general. While another aspect, i.e., whether the value of the force can provide a positive effect on virtual assembly operation, such as a better immersion feeling, is subject to the below judgment from the participants.

4.3.3 Evaluation of the effect of force rendering

After completing all the experiments, the participants are requested to give a score in the range 1–10 (the higher the better) to the three evaluation factors mentioned above. The first evaluation factor, immersion of the VA system, is scored without assembly force feedback and with assembly force feedback (a general feeling from B1, B2, and B3) separately to provide a comparison. The maximum, minimum, and average scores from the 15 participants are shown in Table 1.

From the results shown in the Table 1, the average score of immersion of the shaft-bushing assembly with force feedback (row no. 2) is better than the one without force feedback (row no. 1), which indicates that most participants consider that the force feedback provided by the system is reasonable and more realistic for such virtual assembly operations.

In order to help the participants for a better comparison on force rendering under different fit type, experiments B1, B2, and B3 are arranged within the same virtual environment, where they conduct the insertion operation with three sets of shaft and bushing for experiments B1, B2, and B3 sequentially. Since each insertion operation is corresponding to one fit type and this information is known to the participant in advance, then they give their evaluation scores on how much they feel like the tolerance state is the fit type told, and this is indicated by the data in row of no. 3. The result is quite promising with the minimum score of 7 and average at 8.1. This means that all participants can tell the fit type by the virtual assembly force rendered.

For the evaluation on the stability and continuity of assembly force feedback, all the participants give a score more than 5 (minimum score is 6) with an average of 7.8; this indicates that the fluctuation of the force output from the prototype system does not affect the immersion feeling of the virtual operation, and most participants acknowledge the continuous and stable force feedback. This is expected due to the introduction of the tolerance control factor. With this continuous changing force feedback based on each of the sampled section along the assembly length, the prototype is able to provide a more realistic feeling on force continuality.

Other than looking at the maximum, minimum, and average scores, the distributions of the score are statistically investigated by their quartiles. As the box-plot in Fig. 9 shows,

Table 2 Times of correct identifications of each experiment

Experiment	Participants															Σ
	A	B	C	D	E	F	G	H	I	J	K	L	M	N	O	
B1	14	12	12	15	14	15	12	14	15	14	14	14	12	15	13	205
B2	11	14	13	12	13	14	9	10	13	10	11	14	10	14	13	181
B3	13	9	13	12	9	12	13	13	10	13	12	10	14	10	11	174

though the Q3 of experiment A3 is above 6 (more than 5, half of the score), which means most of the participants are OK with the feeling of immersion by providing collision detection and geometric constraints during the assembly process, the Q3 of evaluation factor no. 2 is close to a score of 9, a lot more than that of experiment A3. Since the evaluation factor no. 2 is scored with the force feedback provided by the proposed approach, hence it indicates that with the continuous force feedback during VA, most of the participants have a better feeling of immersion. As the quartiles for evaluation factors no. 2, 3, and 4 reveal, their Q3 are all above 8; this is also a quite promising and positive judgment from the participants to the proposed approach.

Furthermore, to get a more objective evaluation on the capability of identifying different fit types, instead of telling the fit type of the experiment in advance, the same group of participants was asked to repeat the operation task 15 times for each specific but unknown fit type. The scene and the operation are set to be identical while the tolerance control factor $B(l_i)$ of each fit type is generated randomly. Moreover, the shape and color of parts are set to be identical. After each of every 15 times of insertion operation, the participant judges the fit types accordingly. Table 2 shows how many times (out of 15) each participant could correctly distinguish or identify the fit type.

Since the distribution of the data collected is unknown, it cannot be normalized. Hence, in this study, the Friedman test (non-parametric test) [24] is used to compare the data in Table 2. The level of significance here is selected as $\alpha = 0.05$, which is the common value used to judge whether the data has a significant difference or not. With the data analysis, the p value obtained is $p = 0.013$. It is less than the level of significance selected, which indicates that there is a statistically significant difference between the different fit types. Then the post hoc test is run to find out the difference between each fit types, for which the Wilcoxon signed-rank tests with Bonferroni correction is adopted as the post hoc test method. The level of significance with Bonferroni correction is $\alpha' = 0.017$. It is used as a criterion to judge the statistical difference between each fit types. The result showed that the clearance fit is not only statistically different from the interference fit ($p_1 = 0.009 < 0.017$), but also from the transition fit ($p_2 = 0.007 < 0.017$). But there is little difference can be found between the interference fit and transition fit ($p_3 = 0.503 > 0.017$). Moreover, from the participants' performance of the assembly operation, the overall value of B1 is 205 (as shown in Table 2), which is greater than the value of B2 and B3. This indicates that the performance of identifying the clearance fit is better than the other two fit types. However, though the correct identification times with the interference fit is slightly higher than that of the transition fit, the result of post hoc test did not reveal much statistical difference between them.

From the results, it can be found that participants can tell the clearance fit with VA operations. This is due to the fact that the clearance between the mating parts is obvious to be sensed and the assembly force based on the Coulomb friction model is more reasonable and close to the operation in the real world. On the other hand, due to the hardware limitation of the force output magnitude of the haptic device, after mapping the force magnitude to the acceptable range of the haptic device interface, the difference between the variations of the assembly force under the interference fit and the transition fit is difficult to tell and not easily to be sensed.

5 Conclusion

Integrating force feedback with virtual assembly system can help users feel the virtual parts and better understand assembly operations. More specifically, for mechanical assembly, the force required for assembling two parts is highly dependent on their tolerance design. Other than providing a constant force, this work presents a novel approach of force rendering for virtual assembly of mechanical parts. It features a force rendering algorithm that takes into account the three common mechanical fit types with continuous tolerance variation between the mating surfaces. Moreover, the approach is developed into a prototype VA system, with which the case studies on a typical mechanical shaft-bushing assembly are conducted. The results have shown that the force rendered is output continuously and more realistic to users and the user performance is acceptable. Not only the immersion feeling of users is enhanced by the force feedback but also they are able to identify the different fit types so as to allow possible evaluation on the tolerance design of the assembly.

Acknowledgments This work was partially supported by the Nature Science Foundation of China (grant number 51275177), the Science & Technology Research Program of Guangdong (grant number 2015A030401028), and the New Century Excellent Talents Program of China (grant number NCET-12-0197).

References

1. Jarayam S, Connacher HI, Lyons KW (1997) Virtual assembly using virtual reality techniques. Comput Aided Des 29(8):575–584
2. Gao W, Shao XD, Liu HL (2014) Virtual assembly planning and assembly-oriented quantitative evaluation of product assemblability. Int J Adv Manuf Technol 71:483–496
3. Xia P, Lopes A, Restivo M (2011) Design and implementation of a haptic-based virtual assembly system. Assem Autom 31(4):369–384
4. Burdea GC (1999) Invited review: the synergy between virtual reality and robotics. IEEE Trans Robot Autom 15(3):400–410

5. Volkov SA, Vance JM (2001) Effectiveness of haptic sensation for the evaluation of virtual prototypes. Proc ASME Des Eng Tech Conf 2:1151–1160
6. Coutee AS, Bras B (2004) An experiment on weight sensation in real and virtual environments. Proc ASME Des Eng Tech Conf 4: 225–231
7. Lim T, Ritchie JM, Corney JR, Dewar RG, Schmidt K, Bergsteiner K (2007) Assessment of a haptic virtual assembly system that uses physics-based interactions. ISAM-IEEE Int Symp Assem Manuf 147–153
8. Lim T, Ritchie JM, Dewar RG, Corney JR, Wilkinson P, Calis M, Desmulliez M, Fang JJ (2007) Factors affecting user performance in haptic assembly. Virtual Reality 11(4):241–252
9. Coutee AS (2004) Virtual assembly and disassembly analysis: an exploration into virtual object interactions and haptic feedback. Dissertation, Georgia Institute of Technology
10. Seth A, Su HJ, Vance JM (2006) SHARP: a system for haptic assembly & realistic prototyping. Proc ASME Des Eng Tech Conf
11. Seth A, Su HJ, Vance JM (2005) A desktop networked haptic VR interface for mechanical assembly. Am Soc Mech Eng Comput Inf Eng Div CED 10:173–180
12. Iglesias R, Casado S, Gutierrez T, Garcia-Alonso A, Yap KM, Yu W, Marshall A (2006) A peer-to-peer architecture for collaborative haptic assembly. Proc IEEE Int Symp Distrib Simul Real Time Appl DS RT 25–34
13. Tang XQ, Wang B, Wang SC (2010) Quality assurance model in mechanical assembly. Int J Adv Manuf Technol 51:1121–1138
14. Li JR, Wang QH, Huang P, Shen HZ (2010) A novel connector-knowledge-based approach for disassembly precedence constraint generation. Int J Adv Manuf Technol 49:293–304
15. Khodaygan S, Movahhedy MR (2011) Tolerance analysis of assemblies with asymmetric tolerances by unified uncertainty–accumulation model based on fuzzy logic. Int J Adv Manuf Technol 53:777–788
16. Garbaya S, Zaldivar-Colado U (2007) The affect of contact force sensations on user performance in virtual assembly tasks. Virtual Reality 11(4):287–299
17. Robert LM (2008) Machine elements in mechanical design. China Machine Press, Beijing
18. Fortini ET (1967) Dimensioning for interchangeable manufacture. Industrial Press, New York
19. Wilson JR (1997) Virtual environments and ergonomics: needs and opportunities. Ergonomics 40(10):1057–1077
20. Gupta R, Sheridan T, Whitney D (1997) Experiments using multi-modal virtual environments in design for assembly analysis. Presence Teleoper Virtual Environ 6(3):318–338
21. Gupta R, Whitney D, Zeltzer D (1997) Prototyping and design for assembly analysis using multimodal virtual environments. Comput Aided Des 29(8):585–597
22. Xia P, Lopes AM, Restivo MT, Yao Y (2012) A new type haptics-based virtual environment system for assembly training of complex products. Int J Adv Manuf Technol 58(1–4):379–396
23. Kang H, Park YS, Ewing TF, Faulring E, Colgate JE (2004) Visually and haptically augmented teleoperation in D&D tasks using virtual fixtures. Conf Robot Remote Syst Proc 10:466–471
24. Ramos A, Prattichizzo D (2014) Vibrotactile stimuli for distinction of virtual constraints and environment feedback. Lect Notes Comput Sci 8618:141–149